Supporting Information

Performance Enhancement Strategies of Surface Plasmon Resonance Sensors in Direct Glucose Detection using Pristine and Modified UiO-66: Effects of Morphology, Immobilization Technique, and Signal Amplification

Gilang Gumilar[1,2], Joel Henzie[3], Brian Yuliarto[2,4]*, Aep Patah[5], Nugraha Nugraha[2,4], Muhammad Iqbal[2,3], Mohammed A. Amin[6,] Md. Shariar A. Hossain[7,8], Yusuke Yamauchi[3,8], Yusuf Valentino Kaneti[8]**

[1] *Welding and Fabrication Engineering Technology Department, Institut Teknologi Sains Bandung, Central Cikarang, Bekasi 17530, Indonesia*

[2] *Advanced Functional Materials (AFM) Laboratory, Engineering Physics Department, Institut Teknologi Bandung, Bandung 40132, Indonesia*

[3] *JST-ERATO Yamauchi Materials Space-Tectonics Project and International Center for Materials Nanoarchitectonics (WPI-MANA), National Institute for Materials Science (NIMS), 1-1 Namiki, Tsukuba, Ibaraki 305-0044, Japan*

[4] *Research Center for Nanoscience and Nanotechnology (RCNN), Institut Teknologi Bandung, Bandung 40132, Indonesia*

[5] *Inorganic & Physical Chemistry Research Division, Institut Teknologi Bandung, Bandung 40132, Indonesia*

[6] *Department of Chemistry, College of Science, Taif University, P. O. Box 11099, Taif 21194, Saudi Arabia*

[7] *School of Mechanical and Mining Engineering, The University of Queensland, St. Lucia, QLD 4067, Australia*

[8] *School of Chemical Engineering and Australian Institute for Bioengineering and Nanotechnology (AIBN), The University of Queensland, St. Lucia, QLD 4072, Australia*

E-mails: gilang.gumilar@itsb.ac.id; brian@tf.itb.ac.id; v.kaneti@uq.edu.au

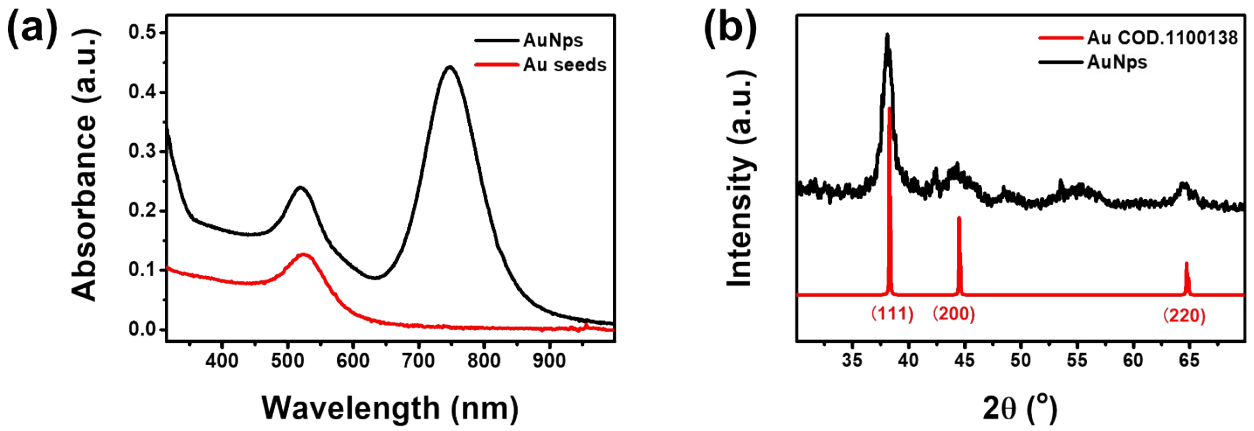

Fig. S1. (a) UV-vis spectra of Au seeds and AuNps, and (b) XRD patterns of synthesized AuNps and simulated Au [obtained from crystallography open database (COD) No.1100138].

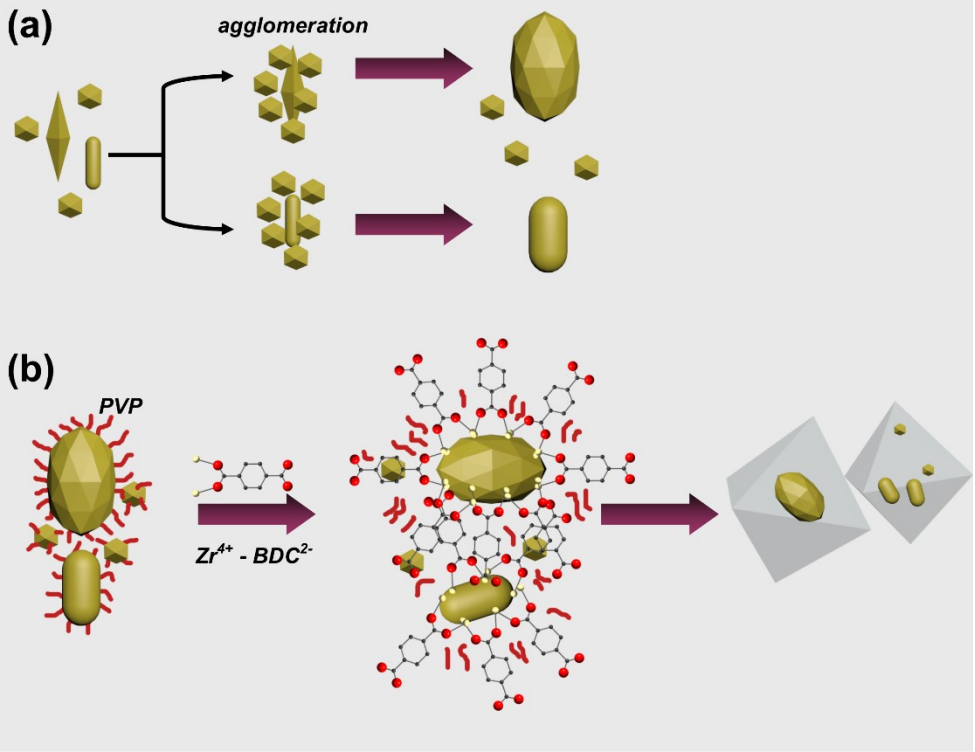

Fig. S2. (a) The possible transformation scheme of AuNps and (b) the hybridization process of UiO-66 with AuNps.

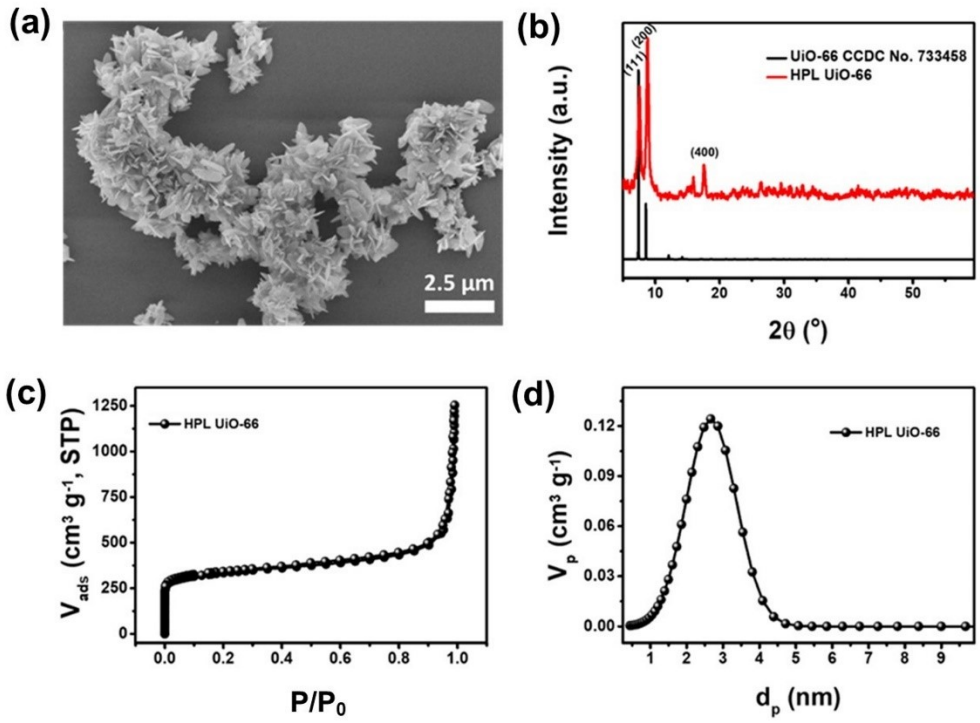

Fig. S3. (a) SEM image of HPL UiO-66. (b) XRD patterns of HPL UiO-66 and simulated UiO-66 from Cambridge Crystallographic Data Centre (CCDC) No. 733458. (c) N_2 adsorption-desorption isotherm and (d) NLDFT pore distribution plot of HPL UiO-66.

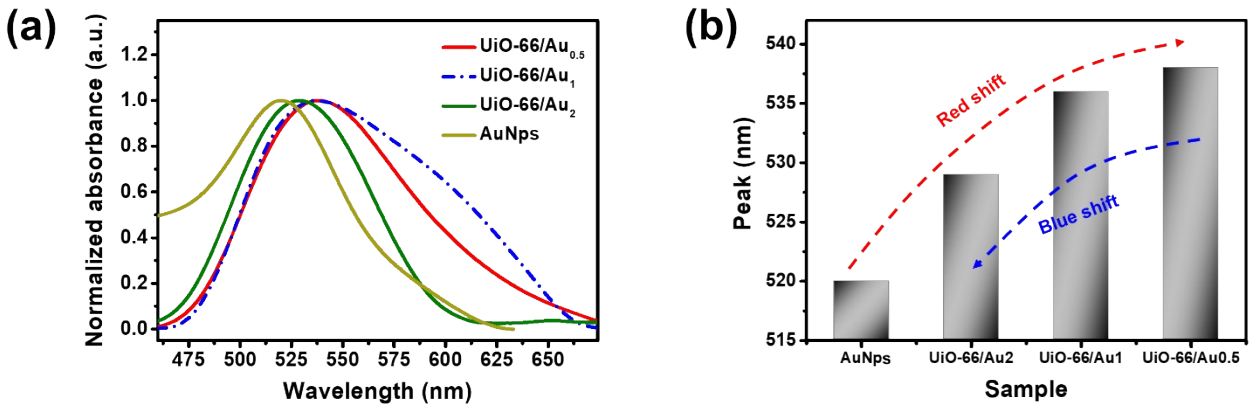

Fig. S4. (a) Normalized UV-vis absorption spectra of AuNps and UiO-66/Au samples in the wavelength range of 460-700 nm, showing the LSPR peak broadening. (b) The bar chart diagram of the LSPR peak position of AuNp and UiO-66/Au, showing the LSPR peak shifts.

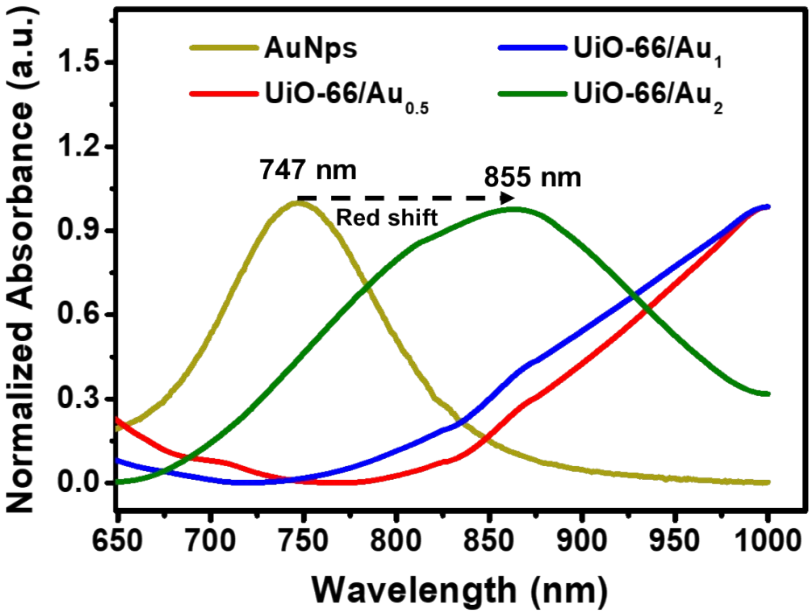

Fig. S5. Normalized UV-vis absorption spectra of AuNps and UiO-66/Au samples in the wavelength range of 650-1000 nm, showing the LSPR peak shifting and broadening.

Table S1. Refined lattice parameters of UiO-66 and UiO-66/Au samples from Rietveld refinement and the strain values of UiO-66 before and after hybridization with AuNps.

Sample	*a* (Å)	ϵ
UiO-66	20.7795	0.000294
UiO-66/$Au_{0.5}$	20.7439	0.00256
UiO-66/Au_1	20.7447	0.00392
UiO-66/Au_2	20.7646	0.00212

Table S2. The ΔRU values of the SPR sensor functionalized with HPL UiO-66/SC, UiO-66/SC, and UiO-66/DA for glucose detection in the concentration range of 0.1-10 mM.

Sample	ΔRU for glucose concentration					
	0.1 mM	0.5 mM	1 mM	2.5 mM	5 mM	10 mM
HPLUiO-66/SC	2.861	3.612	4.444	6.994	10.903	21.736
UiO-66/SC	2.805	4.761	7.237	12.419	22.7402	27.415
UiO-66/DA	6.921	10.539	13.453	21.644	24.842	24.709

Table S3. The ΔRU values of the SPR sensor functionalized with UiO-66, UiO-66/$Au_{0.5}$, UiO-66/Au_1, and UiO-66/Au_2 for glucose detection in the concentration range of 0.1-10 mM.

Sample	ΔRU for glucose concentration (mM)							
	0.01	**0.05**	**0.1**	**0.5**	**1**	**2.5**	**5**	**10**
UiO-66	-	5.218	6.921	10.539	13.4523	21.644	24.842	24.709
UiO-66/$Au_{0.5}$	3.394	8.152	12.073	15.240	16.589	18.604	21.3474	24.429
UiO-66/Au_1	0.609	2.305	6.8403	8.588	9.879	13.114	14.448	15.503
UiO-66/Au_2	1.224	1.788	2.820	4.189	5.585	7.641	10.130	13.023

Table S4. The ΔRU values of glucose detection in PBS and human serum + PBS solutions using UiO-66/$Au_{0.5}$.

Concentration (mM)	**ΔRU**		**Recovery (%)**
	PBS	Human serum + PBS	
0.01	3.39429	1.273279	37.51238
0.05	8.1521	6.48006	79.48946
0.1	12.07335	9.70265	80.36419
0.5	15.24018	12.68718	83.24823
1	16.58947	14.97328	90.25774
2.5	18.60416	19.4169	104.3686
5	21.34749	22.13525	103.6902
10	24.42883	23.96072	98.08378

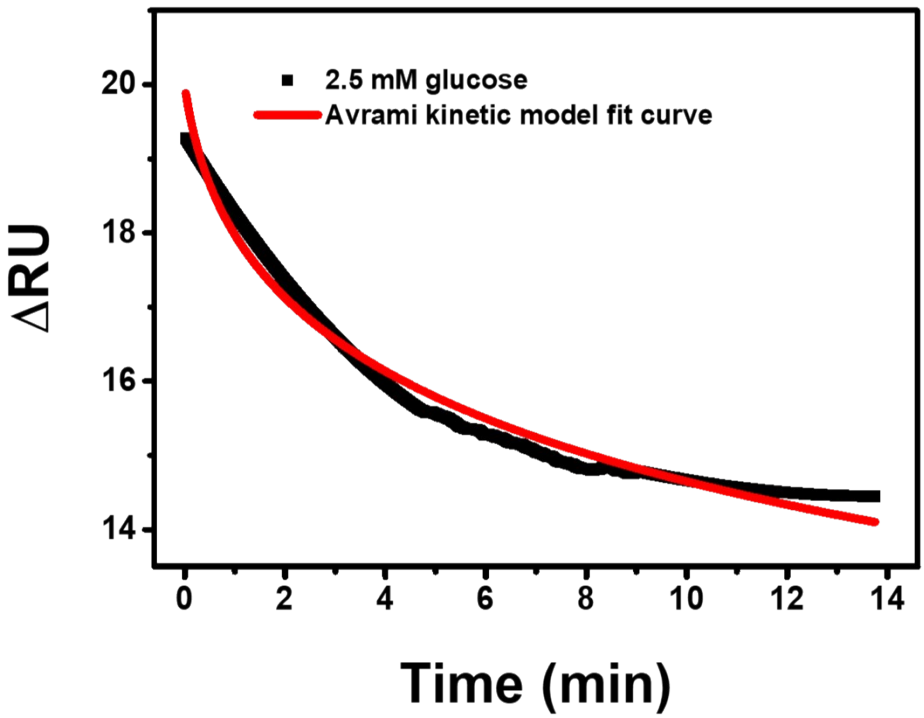

Fig. S6. The non-linear fitting curve of Avrami's kinetic adsorption model on 2.5 mM glucose dissociation experimental data of UiO-66/$Au_{0.5}$.